chemosensors

MDPI

Article

Plasma-Polymerized Thiophene-Reduced Graphene Oxide Composite Film Sensor for Ammonia/Amine Detection at Room Temperature

Baliram Nadekar [1], Yogesh B. Khollam [2], Shoyebmohamad F. Shaikh [3], Ajinkya Trimukhe [4], Rajendra Deshmukh [4], Pravin S. More [1,*], Muhammad Usman Hassan Siddiqui [5], Abu ul Hassan S. Rana [6,*] and Marimuthu Palaniswami [6]

[1] Nanomaterials Application Laboratory, Department of Physics, The Institute of Science, Madam Cama Road, Fort, Mumbai 400032, Maharashtra, India
[2] Research Centre in Physics, Department of Physics, Baburaoji Gholap College, Sangvi, Pune 411027, Maharashtra, India
[3] Department of Chemistry, College of Science, Bld-5, King Saud University, Riyadh 11451, Saudi Arabia
[4] Department of Physics, Institute of Chemical Technology, Matunga, Mumbai 400019, Maharashtra, India
[5] Unilever Lipton Jebal Ali Factory Engineering Department, Dubai P.O. Box 325, United Arab Emirates
[6] Department of Electrical and Electronic Engineering, The University of Melbourne, Parkville 3010, Australia
* Correspondence: pravin.more@iscm.ac.in (P.S.M.); a.rana@unimelb.edu.au (A.u.H.S.R.)

Abstract: Industrialization has led to an increasing need for specific and selective gas sensors in the past few decades. Environmental monitoring of certain volatile compounds such as ammonia is necessary. Advancements in the food storage sector have created the need for cheap and effective amine chemosensors. Classical chemosensors still face several issues, such as a lack of selectivity and low sensitivity toward ammonia and amines. Sensitivity is defined as the relative change in response expressed in percentage. In this work, we have resolved a few issues associated with the ammonia and amine sensors, such as low selectivity, long-term instability, and unreliability under higher temperatures using plasma-polymerized thiophene (PPTh) reduced graphene oxide (rGO) composite films. PPTh films were prepared using RF plasma polymerization with optimized deposition parameters. Several samples were evaluated for their sensing response to understand the optimal PPTh and rGO ratio in the PPTh-rGO composite. These composite PPTh-rGO films have shown 4 times higher sensitivity for ammonia/amines than individual PPTh and rGO films. Ammonia, methylamine (MA), dimethylamine (DMA), and trimethylamine (TMA) were primary analytes and tested for sensing response of the PPTh-rGO composite. The sensitivity measured ranges from 1328 for trimethylamine to 2354 for methylamine at 1000 ppm. The order of sensitivity was found to be MA > Ammonia > DMA > TMA. Polymer swelling, reduced charge carriers, and disruption of conductive pathways can explain possible sensing mechanisms. PPTh-rGO composite films have shown selectivity as high as 110 for ammonia/amine over other commonly used volatile organic compounds. The sensing response of these films is stable for any temperature fluctuations from 30 °C to 150 °C. Additionally, films showed stable sensitivity for over 4 months. Thus, composite films of PPTh-rGO can be effectively used to develop highly selective and stable gas sensors for the environmental monitoring of ammonia/amines.

Keywords: thiophene; reduced graphene oxide; thin film; room temperature sensing; ammonia gas sensors; electronic nose

Citation: Nadekar, B.; Khollam, Y.B.; Shaikh, S.F.; Trimukhe, A.; Deshmukh, R.; More, P.S.; Siddiqui, M.U.H.; Rana, A.u.H.S.; Palaniswami, M. Plasma-Polymerized Thiophene-Reduced Graphene Oxide Composite Film Sensor for Ammonia/Amine Detection at Room Temperature. *Chemosensors* **2023**, *11*, 42. https://doi.org/10.3390/chemosensors11010042

Academic Editors: Manuel Aleixandre and Jun Wang

Received: 28 October 2022
Revised: 22 December 2022
Accepted: 29 December 2022
Published: 3 January 2023

1. Introduction

The Industrial advancement in the last few decades has led to excessive consumption of chemicals as raw materials. Storing and transporting these chemicals have created disasters in recent history. These industries also produce organic waste products that harm

the environment surrounding living species [1]. Detecting and controlling the presence of these organic chemicals, especially volatile compounds, is important for a sustainable future. Additionally, food quality monitoring is another area where sensing volatile compounds are necessary. Amine chemosensors play an important role in minimizing food wastage in transport and storage. Early detection of these amines would enable the safe consumption of high-protein foods [2]. Ammonia sensing is a widely explored field, and many effective ammonia sensors are available in the market. On the other hand, amines sensing did not receive enough attention from researchers. Traditional methods used for amine sensing include liquid chromatography, gas chromatography combined with mass spectroscopy, and fluorometric analysis [3]. These are sophisticated methods for analytical measurements. They are reliable and provide accurate measurements of the amine concentration, but these methods are not suitable for easy operations due to their long testing time and elaborate procedure. Currently, work is being done to develop easy-to-operate, selective, and sensitive amine chemosensors [4]. Chemiresistive sensors are one such option that has been applied in the field of gas sensing for decades, sensing various gases. Sensing volatile compounds using chemiresistive sensors is easy and cheap. Traditionally, metal oxide-based chemiresistive gas sensors were the most common. However, the need for better sensing abilities has pushed scientists to look for new materials with different chemosensing abilities [5]. Recently, conducting polymer and composite-based gas sensors have offered enhanced sensitivity and high selectivity for different gases [6].

Operating at room temperature, these polymer-based chemiresistive gas sensors are better than metal oxide-based chemiresistive gas sensors. Polymer synthesis is easily possible via various existing polymerization methods. Chemical polymerization is a more commonly used method for polymerization. It is an easy method, but it produces harmful byproducts that pollute the environment. While looking out for a sustainable future, we must adopt practices that do not harm the environment. Plasma polymerization is one such technique used for polymerization. It does not involve any solvent; hence, no harmful byproducts are generated in the process. Cold plasma or electrical plasma polymerization only uses electrical energy for polymerization. Additionally, this method is already employed in the mass manufacturing of thin films [7]. Plasma polymerization produces polymers that can differ in chemical and electrical properties from chemically synthesized polymers. This provides a unique opportunity to explore all possible applications of plasma polymers. Reduced graphene oxide (rGO) is another material used in sensor films [8]. rGO is a form of graphene with similar electrical properties. rGO has a far less complicated and easy synthesis process than single-layer graphene. Synthesis involves the reductive processing of graphene oxide by chemical, thermal, microwave, or photo-chemical methods to reduce its oxygen content [9]. Some major problems current ammonia/amine sensors face are lack of selectivity and low sensitivity. Some of the sensors can deteriorate if operated for a longer period. Metal oxide-based ammonia/amine sensors are needed to be operated at high temperatures. Maintaining sensors at high temperatures is not cost-effective.

Previously, polythiophene and its derivatives were synthesized by chemical polymerization and deposited via various gas sensing methods. Bo Li and team developed a chemical sensor array using polythiophene where they recorded sensitivity ranging from 6.39 for methanol to 9.25 for methylene chloride at 1000 ppm each. This array was able to differentiate between various common VOCs [10]. V.C. Goncalves et al. published their research on detecting volatile organic chemicals using polythiophene derivatives at the sensing layer. In contrast, they found that n-hexane at a concentration of 1000 ppm had a sensitivity of 8 [11]. A highly effective polythiophene sensor was developed by Choon-Sang Park, to deliver a sensitivity of 73 for 1ppm of NO_2. They used atmospheric plasma to fabricate polythiophene films and iodine doping to enhance conductivity [12]. Their efforts highlight the importance of applying polythiophene film for highly sensitive gas sensors and exploring specific gases. Ruijie Zhang and team recently published their work on mesoporous cellulose nanofibers-interlaced PEDOT: PSS hybrids for chemo-resistive ammonia detection. They reported a sensitivity of 7.46/ppm for ammonia concentrations

below 3 ppm. This chemoresistive sensor operated at 25 °C and 55% relative humidity. For 1 ppm of ammonia, they recorded a fast response/recovery time of 4.9 s/5.2 s. This device is ideal for low power consumption, super fast response, and enhanced sensitivity [13]. In the present work, we have focused on developing highly selective ammonia/amine sensing films that can have stable sensitivity months after fabrication or first use. Plasma-polymerized polythiophene (PPTh) and rGO composite chemosensing films were fabricated using plasma polymerization and ultrasonic spray deposition. We have studied the sensing response of these films for ammonia, methylamine (MA), dimethylamine (DMA), and trimethylamine (TMA). These films could be directly used as a chemoresistive sensor or a sensing layer in a transistor-based gas sensor.

2. Materials and Methods

2.1. Materials and Chemicals

Hydrazine hydrate (H_2N_4), Hydrogen peroxide (H_2O_2), potassium permanganate ($KMnO_4$), sulfuric acid (H_2SO_4), hydrochloric acid (HCl), nitric acid (HNO_3) sodium nitrate ($NaNO_2$) and pristine vein graphite were obtained from Sigma-Aldrich. All the VOCs and thiophene (monomer) were obtained from SD fine chem ltd. All the chemicals were AR grade (>99% purity) and used as received without any further purification. Glass substrates were obtained from Polar Industries, Mumbai. A thorough cleaning process was used to prepare substrates before deposition. Deionized water, isopropyl alcohol, and toluene were used to clean the substrates.

2.2. PPTh Polymerization, rGO Synthesis, and Composite PVAc-rGO

Plasma polymerization was carried out using a home-built parallel plate RF plasma polymerization system. Polymerization was powered by a Tektronix RF power source of 2 kV and an RF frequency of 13.6 MHz. The factors affecting deposited film quality include monomer flow, the distance between parallel plate electrodes, electric power applied using an RF source, frequency of pulsed plasma, duty cycle, and total deposition time. The monomer flow rate was optimized to maintain the chamber pressure below 10^{-3} Torr to 10^{-2} Torr. Pulsed plasma was used during the present deposition process instead of continuous plasma as continuous plasma could burn monomer material even at moderately high power [14]. The pulse frequency varied between 5 Hz to 100 Hz with different duty cycles to deposit test samples and optimize deposition parameters. The total deposition time was kept constant at 5 min for every sample. Four finalized samples were selected with the following parameters and identified as described in Table 1.

Table 1. Deposition parameters for different plasma-polymerized samples.

Sr. No.	Sample Name	Frequency	Duty Cycle	Total Deposition Time
1	PT1	10 Hz	50%	5 min
2	PT2	10 Hz	10%	5 min
3	PT3	20 Hz	50%	5 min
4	PT4	20 Hz	10%	5 min

These PPTh samples may not be conducive in their as-deposited state. To overcome this issue, some form of doping is often introduced into them [15]. We have used iodine doping to enhance the conductivity of PPTh films. Samples were placed in a closed container with 2 g of resublimed iodine. Iodine vapors were used to dope PPTh films to their saturation for 24 h (Figure 1a).

rGO was synthesized through a well-established chemical method called modified Hummer's method. 2.5 g of $NaNO_3$ and 5.0 g of graphite powders were mixed in 100 mL of concentrated H_2SO_4. This mixture was placed in an ice bath to maintain a temperature of 5 °C. 10.0 g of $KMnO_4$ was gradually added to the mixture while stirring it [16,17]. The mixture was added to 230 mL of water and held at a temperature of 60 °C for 30 min. The

oxidation reaction was terminated by cooling the mixture to room temperature and adding 30% H_2O_2 solution to the mixture. Then, the mixture was filtered and washed several times with 5% HCl and double distilled water. Later, the mixture was dried in a vacuum oven for 24 h to obtain graphene oxide (GO) powder [18–20]. The rGO was prepared by reducing GO with sodium borohydride ($NaBH_4$) (Figure 1b). Ultrasonic spray deposition was used to fabricate composite films of PPTh and rGO. Primarily, different weighted concentrations of rGO were dispersed in 50 mL of deionized water. The colloid was sprayed over PPTh films using an ultrasonic spray gun. A hot plate was used to assist in the evaporation of the dispersed medium. Using the sensing response of as-deposited PPTh films (see Section 3.4.1), PT2 was selected for rGO variation studies. The following parameters were used to deposit primary composite samples. (Table 2)

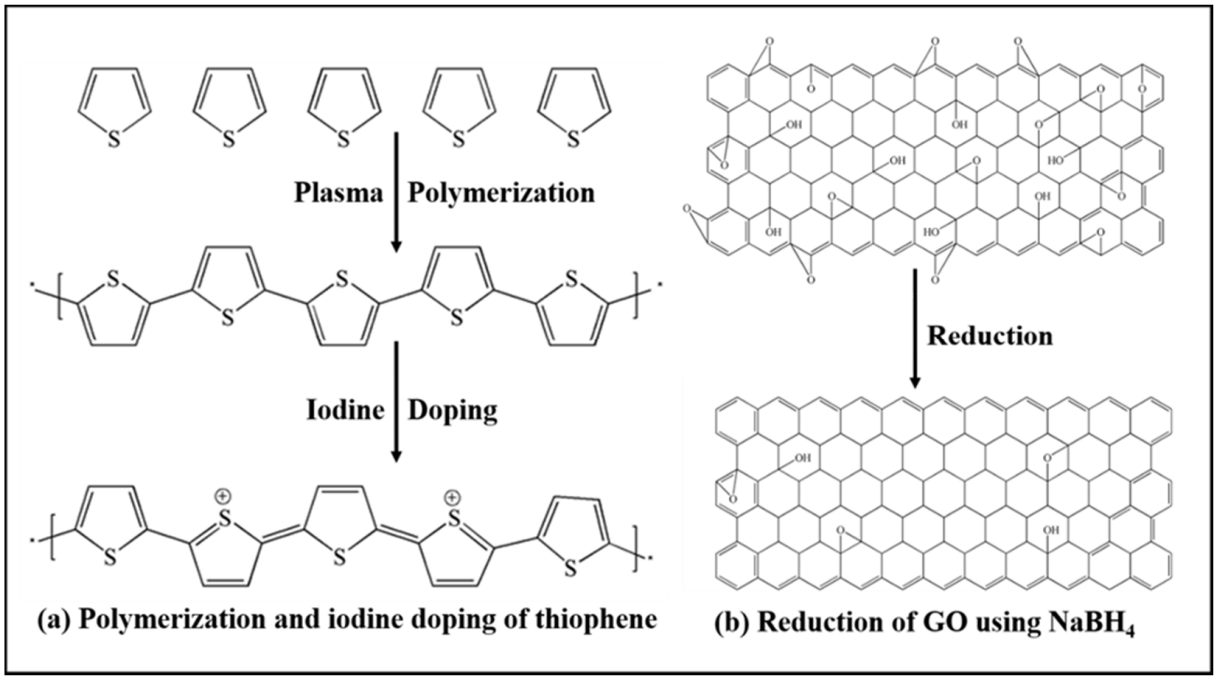

Figure 1. (**a**) Chemical structure of thiophene, PPTh, and iodine-doped PPTh, (**b**) GO and rGO.

Table 2. Name and constituents of primary PPTh-rGO composite.

Sr. No.	Composite Sample Name	PPTh Sample Used	rGO Concentration (in DI Water)
1	PT2G1	PT2	0.01 g/50 mL
2	PT2G2	PT2	0.1 g/50 mL
3	PT2G3	PT2	1.0 g/50 mL
4	PT2G4	PT2	10 g/50 mL

Sensing results from these samples (see Section 3.4.1) were used to decide the rGO concentration in the final four composite samples. The final samples are named PT1G3, PT2G3, PT3G3, and PT4G3. (Table 3).

Table 3. Name and constituents of final PPTh-rGO composite.

Sr. No.	Composite Sample Name	PPTh Sample Used	rGO Concentration (in DI Water)
1	PT1G3	PT1	1.0 g/50 mL
2	PT2G3	PT2	1.0 g/50 mL
3	PT3G3	PT3	1.0 g/50 mL
4	PT4G3	PT4	1.0 g/50 mL

2.3. Structural, Chemical, and Morphological Studies

JEOL (JSM-IT300LV) scanning electron microscope was used to study the surface morphology of PPTh-rGO composite films. The elemental analysis and the study of functional groups were done using Perkin Elmer Spectrum Two FTIR. Film samples were directly placed on the diamond crystal of FTIR to record spectra with an air background. XRD patterns were recorded within 2θ range of 10°–60° using an XPERT-PROMPD X-ray diffractometer (CuKα radiation, λ = 1.5405 Å). For higher magnification images, FE-SEM (Nova NanoSEM 450) was used.

2.4. Ammonia/Amine Sensing Characteristics

Home built four probe-based gas sensing system that was used to study the sensing response of PPTh, rGO, and PPTh-rGO composite films. The sensing mechanism allows polymer materials to show gas sensing response at room temperatures [6]. Hence, all the sensing studies were carried out at room temperature except for temperature stability. Keithley source meter 2400 was operated with a current compliance of 0.01 A for recording resistivity readings. Sourced voltage was kept below 5 V throughout the sensing studies [21]. Samples were mainly studied for their sensing response towards the ammonia (NH_3), methylamine (MA), dimethylamine (DMA), and trimethylamine (TMA). To understand the selectivity of samples in the presence of other VOCs, they were also tested for VOCs, such as acetone, benzene, toluene, and dichloromethane. The repeatability of the sensing response was studied by recording the number of sensing cycles for single sample-gas pair [22]. PPTh-rGO composite sample with the best sensing response was studied for its temperature stability between 30 °C to 150 °C. The long-term stability of the same sample was studied by observing its sensing response for 4 months. Then, the sensing response was studied at various VOC concentrations to understand how sensitivity varies with the gas concentration. *Selectivity* was calculated as a ratio of *sensitivities* [17].

$$Sensitivity = \left| \frac{R_a - R_g}{R_a} \right| \times 100$$

$$Selectivity = \frac{S_{g1}}{S_{g2}}$$

R_a and R_g are the resistances of the film in the presence of air and gas 'g', respectively. S_{g1} and S_{g2} are sensitivities for gas 1 and gas 2.

3. Results and Discussion

3.1. Structural Analysis

XRD spectra reveal structural information about the fabricated films. Figure S1a shows the XRD spectra of as-deposited PPTh samples PT1, PT2, PT3, and PT4. It shows a broad peak from 2θ = 12.70° to 2θ = 39.26°. No significant sharp peak is observed in the XRD pattern of as-deposited PPTh films. The absence of any sharp peak in the XRD spectra indicates the amorphous nature of the fabricated PPTh films [23]. A broad peak indicates some form of repeated structure along the X-axis. All as-deposited PPTh films show similar XRD patterns, indicating no major structural difference between different PPTh samples deposited using different deposition parameters. Figure 2a represents the XRD spectra of as-deposited PPTh films PT1, rGO film, and final PPTh-rGO composite films PT1G3, PT2G3, PT3G3, and PT4G3. The XRD pattern of rGO shows a peak at 2θ = 26.60° (002), corresponding to an interlayer distance of 0.339 nm. This is the characteristic peak for rGO [24]. A great extent of exfoliation of GO is responsible for this peak. The synthesized product consists of a few-layer rGO and has a different lattice structure from graphite and GO. rGO films show amorphous nature with a hexagonal structure having orientation along the (002) plane [17]. XRD spectra of the final PPTh-rGO film samples are very similar (Figure 2a). Additional peaks are observed in these spectra compared to as-deposited PPTh films. Small peaks at 2θ = 11.9° and 2θ = 14.9° shows iodine reflection. A much more

significant peak is observed at 2θ = 26.50 integrated into the broad peak of amorphous PPTh. This peak belongs to the rGO present in the composite film. This shows that the structures of both PPTh and rGO are incorporated in the PPTh-rGO composite films.

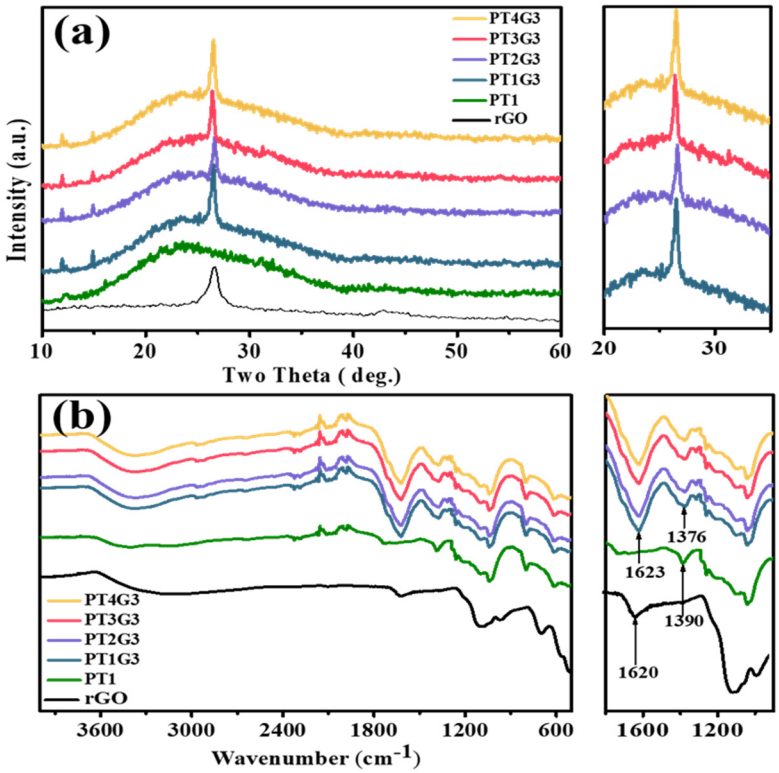

Figure 2. (**a**) XRD spectra of rGO powder, as deposited PPTh sample PT1 and final PPTh-rGO composite samples PT1G3, PT2G3, PT3G3, and PT4G3, (**b**) FTIR spectra of rGO powder, as deposited PPTh sample P1 and final PPTh-rGO composite samples PT1G3, PT2G3, PT3G3, and PT4G3.

3.2. FTIR Analysis

FTIR spectra of plasma-polymerized materials can show reduced or shifted peaks. High power applied during plasma polymerization can generate heavily fragmented polymer chains resulting in shifted FTIR peaks. Figure 2b shows the FTIR spectra of as-deposited PPTh sample PT1, rGO powder, and PPTh-rGO composite samples PT1G3, PT2G3, PT3G3, and PT4G3. Characteristic peaks of PPTh can be observed at 1041 cm^{-1} and 1390 cm^{-1}. These peaks represent stretching vibrations of the thiophene ring [25]. The peak at 1041 cm^{-1} and 1262 cm^{-1}, represent sulfur-oxygen and carbon-oxygen bonds in polythiophene. Peaks identify C=C bonding at 618 cm^{-1} and 900 cm^{-1}. The methyl and methylene groups are represented by peaks at 2928 cm^{-1} and 2963 cm^{-1}. In FTIR spectra, a broad peak at 3140 cm^{-1} corresponds to -OH stretching vibrations of the C-OH group and water content in the material. DI water was used to form a colloid of rGO during ultrasonic spray deposition. Few of these water molecules could be trapped in the polymer film contributing to the -OH peak. The Peak present at 615 cm^{-1} could be attributed to the weak interactions of iodine with PPTh. C=C characteristic peak of rGO is observed at 1620 cm^{-1} belonging to skeleton vibrations of rGO [17]. FTIR spectra of PPTh-rGO composite films show small shifts of two major peaks. The peak located at 1390 cm^{-1} belonging to stretching vibrations of the thiophene ring has shifted to 1376 cm^{-1}. The characteristic peak of rGO at 1620 cm^{-1} is shifted to 1623 cm^{-1}. Generally, a shift to a lower wavenumber will indicate the increased bond length and vice versa [26]. High electronegativity of the rGO molecules could be responsible for this increased bond length in the thiophene ring of PPTh. These shifted peaks indicate the effective composite formation of PPTh and rGO.

3.3. Morphological Analysis

The gas-sensing abilities of the material films are greatly influenced by their surface morphologies. As the specific gases interact with the film surface, their electric response is directly proportional to the amount of gas interacting with the film via the exposed surface. For effective gas sensing applications, film morphology has to assist in maximum gas adsorption. In the case of PPTh-rGO composite films, morphological studies offer a reason for the superiority of composite film PT2G3 in gas sensing activity. Figure 3 shows the SEM images of as-deposited PPTh sample PT1 (Figure 3a), rGO film (Figure 3b), and PPTh-rGO composite films- PT2G1 (Figure 3c), PT2G2 (Figure 3d), PT2G3 (Figure 3e) and PT2G4 (Figure 3f). Composite films have uniform base layers formed by polymer material with some granular structures. Uniform surfaces do not offer a large area for the gas to interact with the material. Hence, films with a uniform surfaces are not very effective in gas sensing [27]. This could be the reason for the low sensitivity observed in the case of as-deposited PPTh films for ammonia/amine sensing. rGO films show wrinkled sheet-like morphology. These surfaces are effective in physically trapping gas molecules [17]. SEM images of composite samples prepared with PT2 and an increasing amount of rGO are shown in Figure 3c–f. As seen in Figure 3c, the least amount of rGO is present on the film surface of PT2G1. In the case of PT2G2, this amount is slightly increased. Still, these rGO sheets do not considerably cover enough surface area to affect the film's sensing ability.

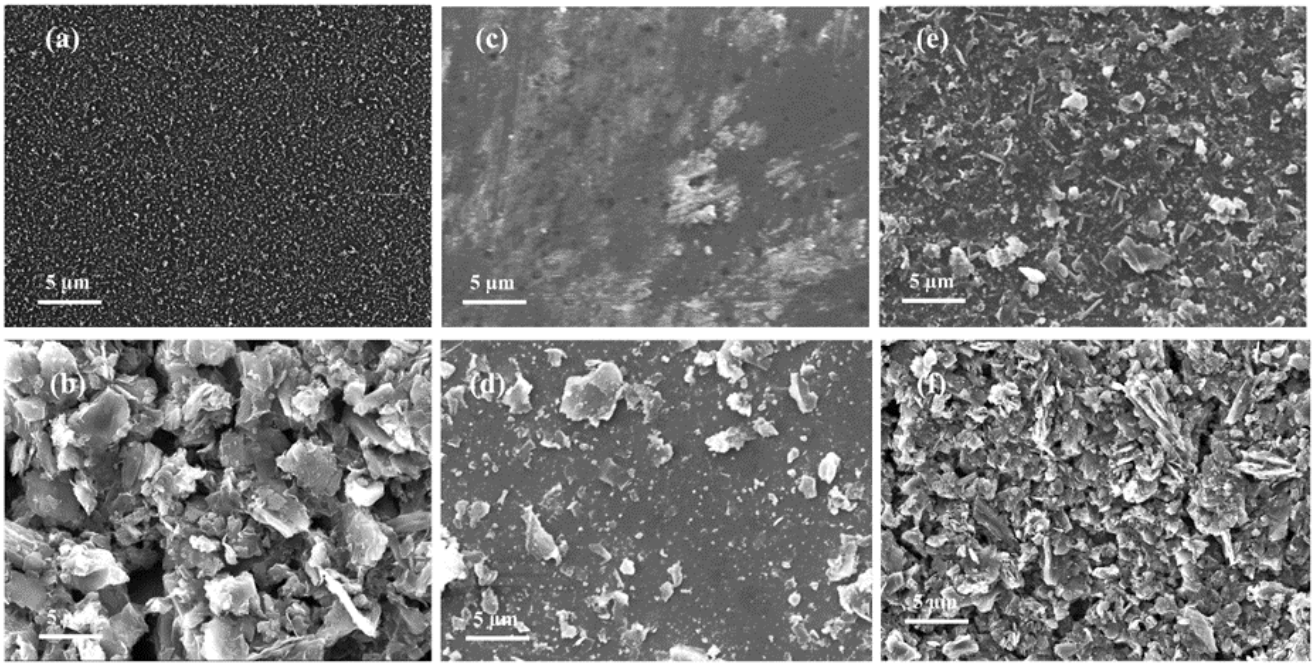

Figure 3. SEM images of (**a**) as deposited PPTh film PT1, (**b**) rGO powder; and PPTh-rGO composite films (**c**) PT2G1; (**d**) PT2G2; (**e**) PT2G3; (**f**) PT2G4.

Hence, the sensing response of PT2G1 and PT2G2 is similar to as-deposited PT2 samples, as most of the analyte gas is still exposed to the base polymer film. In SEM images of PT2G3, a thin layer of rGO covers the entire surface area. As seen in gas sensing results (see Section 3.4.1), this enables PT2G3 films to produce maximum sensitivity in ammonia/amine sensing. As we increase rGO concentration above this point in PT2G4, a thick layer of rGO starts forming on the surface, and the base polymer layer is completely cut off from participating in the sensing process. Hence, the sensing response of PT2G4 is similar to rGO film. Morphological studies provide acceptable reasoning for gas sensing results observed for samples with increasing rGO concentrations. These results emphasize the role of rGO in the gas-sensing process.

3.4. Ammonia/Amine Sensing Studies

3.4.1. Sensitivities of PPTh, rGO, and Composite PPTh-rGO Films

As deposited, PPTh samples were tested for their sensing response towards ammonia/amines at room temperature, and results are plotted in Figure 4a. These readings were recorded at 1000 ppm of each ammonia, MA, DMA, and TMA. Sample PT2 showed the highest sensitivity in the range of 300 to 550 for ammonia/amines under study. PT4 has a similar sensing response, recording sensitivity in the range of 250 to 450 for the same analyte. The sensing repose of PT1 and PT3 is on the lower side. Possible reasons for this could be a difference in the deposition parameters of these samples. The high-duty cycle used for depositing PT1 and PT3 could have resulted in higher fragmentation. rGO film has shown the highest sensitivity of 146 for ammonia. Order of sensitivity for rGO films is ammonia > MA > DMA > TMA. The sensitivity of rGO seems to be decreasing with the increasing molecular weight of the analyte. Higher molecular weight could influence the amount of analyte physisorbed into rGO films [28].

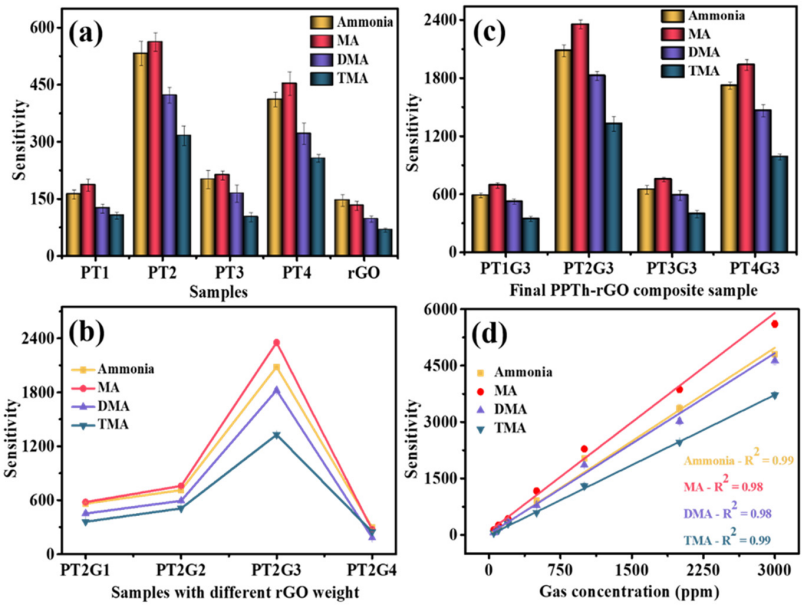

Figure 4. Gas sensing response of (**a**) rGO powder and as deposited PPTh samples PT1, PT2, PT3, and PT4; (**b**) composite samples of PT2 with different rGO weights—PT2G1, PT2G2, PT2G3, and PT2G4; (**c**) final PPTh-rGO composite samples—PT1G3, PT2G3, PT3G3, and PT4G3; (**d**) PT2G3 for varying concentrations of ammonia/amines.

Based on these results, the PT2 sample was used to fabricate primary PPTh-rGO composite samples (Table 2) to optimize the quantity of rGO in composite films. The sensing results of these films are plotted in Figure 4b. The small amount of rGO in PT2G1 and PT2G2 is insufficient to alter the films' sensing response. The PT2G4 thick layer of rGO covers the composite film surface; hence analyte cannot interact with the PPTh in the film. Hence, the sensing response is analogous to rGO films. PT2G3 is the most suitable PPTh-rGO composition observed for sensing activity. rGO concentration in PT2G3 is high enough to impact the sensing mechanism yet not so high; it thickens the entire film surface. Optimized rGO deposition parameters of PT2G3 (1 g of rGO dispersed in 50 mL water) were used to prepare the final composites of each PPTh sample. Samples were named PT1G3, PT2G3, PT3G3, and PT4G3, respectively (Table 3). The sensing results of these samples are presented in Figure 4c. Similar to deposited PPTh film sensing activity, composite film of PT2, i.e., PT2G3, has shown the best results for sensing ammonia/amines at room temperature. The highest sensitivity of 2350 was recorded for MA using these films, and the order of sensitivity is MA > ammonia > DMA > TMA. Results indicate that a composite film's sensitivity is 4 times higher than the maximum sensitivity achieved using as-deposited films. This is a result of the combined effect of PPTh and rGO

materials. The mechanism involved in this sensing activity can be understood in Section 3.4.4. PT2G3 was selected for further in-depth analysis of various sensing characteristics.

In Figure 4d sensing response of PT2G3 is plotted against various concentrations of ammonia/amines at room temperature. The analyte concentration is varied from 50 ppm to 3000 ppm. Generally, gas sensitivity is linearly proportional to the analyte concertation. Hence, linear regression was applied to obtain a calibration curve for PPTh-rGO composite film sample PT2G3. The coefficient of determination was calculated as 0.99 for ammonia, 0.98 for MA, 0.98 for DMA, and 0.99 for TMA. This indicates a good linear fit of a calibration curve.

3.4.2. Repeatability, Response-Recovery Time, and Selectivity

The repeatability of sensors is an important parameter in understanding the reliability of the sensor for commercial operations. Sensors prepared by the same fabrication process should be able to reproduce comparable results under similar working conditions [29]. PPTh-rGO composite sample PT2G3 shows good repeatability (Figure 5a). Sensing results are reproducible with less than 5% error in repeated cycles. The reversibility of the sensor film can be observed in Figure 5a. The sample again reaches the original resistivity in the presence of air at the end of the cycle. This shows the samples can be used for several cycles without any permanent changes in the resistivity [30]. The average response time of the PPTh-rGO films at 1000 ppm of MA was found to be 380 sec simultaneously; recovery time was recorded to be 60 sec. Response time decreases with the concentration of analyte, while recovery time increases with the increasing analyte gas concentration. Figure 5b shows the response and recovery time change as MA concentration increases. Selectivity is a measure to understand if the sensor can differentiate between two different gases. Figure 5c,d shows the selectivity of PPTh-rGO film sample PT2G3 for ammonia/amines and other VOCs (acetone, benzene, toluene, dichloromethane). In the presented study, there are two types of selectivity calculations. First is selectivity among ammonia/amines, and the other is selectivity against other common industrial VOCs. Selectivity values among ammonia/amines range between 0.6 to 1.8 (Figure 5c). This means PPTh-rGO composite films are ineffective in differentiating between ammonia and amines under study. On the other hand, selectivity against other common VOCs is as high as 120 in some cases (Figure 5d). This indicates that PPTh-rGO films are highly selective for ammonia/amines against other common industrial VOCs.

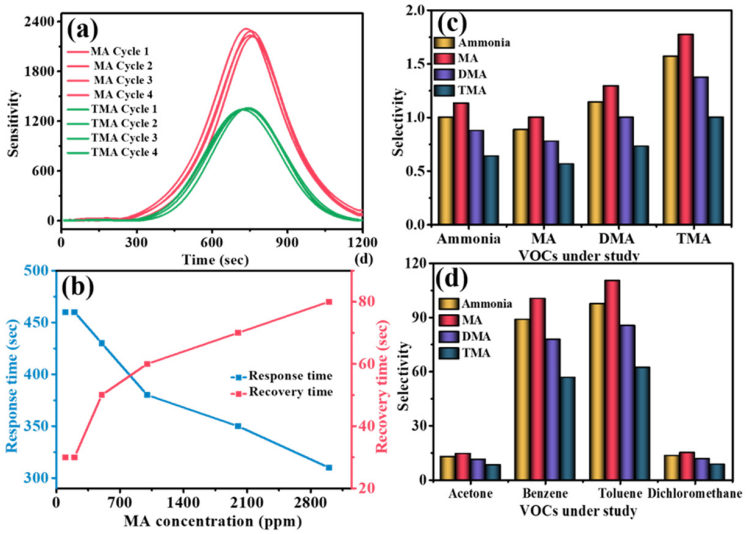

Figure 5. (**a**) Repeatability of PPTh-rGO composite PT2G3 for MA and TMA, (**b**) Response and recovery time of PT2G3 for sensing MA at varying concentrations. (**c**) Selectivity of PPTh-rGO composite sample PT2G3 among ammonia, MA, DMA, and TMA (**d**) Selectivity of PPTh-rGO composite sample PT2G3 for ammonia/amines against other VOCs, such as acetone, benzene, toluene, dichloromethane.

3.4.3. Stability of PPTh-rGO Composite Films under Varying Temperatures, Varied Relative Humidity, and over Long Durations

Polymer-based sensors can operate at room temperature, but to establish independence on the surrounding temperature, the sensor has to be reasonably stable in any temperature fluctuations. The stability of PPTh-rGO films was tested for the temperature range of 30 °C to 150 °C; results are plotted in Figure 6a. PT2G3 sensitivities for ammonia and MA are comparatively stable for the entire range. Some fluctuations in sensitivities are observed in the presence of DMA and TMA. Even though these sensitivities are not ideally constant throughout the temperature range, they neither increase nor decrease with an increment in temperature. Their sensing response is completely independent of the surrounding temperatures. This shows that PT2G3 can be effectively operated at any temperature between 30 °C to 150 °C.

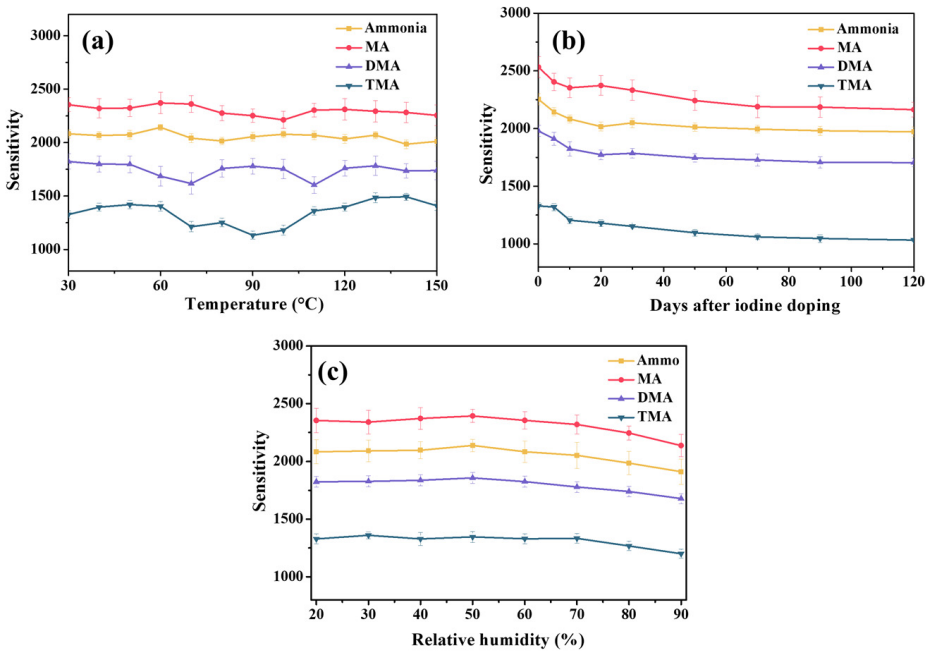

Figure 6. (**a**) Temperature stability of PT2G3 for ammonia/amines sensing (**b**) Long-term stability of PT2G3 for ammonia/amines sensing (**c**) Effect of relative humidity on sensing of PT2G3.

Figure 6b shows the change in sensitivity, recorded for 120 days from initial fabrication. Results indicate that the sensitivity of PT2G3 for ammonia/amines does not change or degrade considerably over 120 days. On day 0, PT2G3 recorded a sensitivity of 2253 for 1000 ppm of ammonia. On day 5, it was reduced to 2144; on day 10 it was recorded to be 2082. This is a 7.5% sensitivity reduction in the 10 days. However, after the first 10 days, ammonia sensitivity is somewhat constant. A 12.5% reduction was recorded for ammonia sensitivity over 120 days. Stability trends can be observed in the case of MA, DMA, and TMA. After 120 days, MA sensitivity was reduced by 14.5%, DMA sensitivity by 14%, and TMA sensitivity by 22%. Major changes in sensitivity are observed in the first 10 days after the deposition. After this period, PPTh-rGO composite films are quite stable for ammonia/amine sensing. This reduction in sensitivity could be caused by interaction between PT2G3 films and various gases present in the surrounding air, as this could result in partial surface contamination of PPTh-rGO films [31].

For room-temperature gas sensors, humidity can affect the gas sensing performance, necessitating warming the sensor before each sample cycle. If the material is hygroscopic then it can affect in presence of the humidity and attains a change in resistance of the sample. Even if the material is non-hygroscopic, humidity affects the sensor surface at ambient conditions causing a low response to gas adsorption reaction. However, for ideal gas sensors changes in relative humidity should not affect sensing performance. Figure 6c

shows the sensing response of PPTh-rGO composite sample PT2G3 for varied relative humidity from 20% to 90%. The sensing response of PT2G3 for ammonia, MA, DMA, and TMA is stable up to 60% of relative humidity, and above 60% of relative humidity, sensitivity for all analyte gases starts reducing linearly. As we reduced relative humidity inside the sensing chamber below 60%, moreover, stable sensing response levels are obtained.

3.4.4. Ammonia/Amine Sensing Mechanism

In the ultrasonic spray deposition method, rGO is carried to the PPTh surface via water droplets. PPTh can absorb these droplets for fraction of the time before water evaporates. Due to this, rGO is placed deeper inside the PPTh surface layers. Figure 7a shows the gas sensing process. In the sensing stage, gas is physisorbed by the material film, which changes the film's resistivity. XRD and SEM studies reveal the amorphous structure of the PPTh-rGO films. Boundaries of these amorphous granules can be highly effective in gas sorption. Accumulating charge carriers at these boundaries can amplify the change in resistivity during the gas-sensing process. Iodine doping in PPTh films increases hole concentration in the material. When ammonia/amine molecules are absorbed in the film surface, their interaction reduces the number of charge carriers available in PPTh film. This reduces conductivity when the sample is exposed to analyte gas (Figure 7b). In pulsed plasma polymerization, the material is deposited layer-wise. The polar hopping process is responsible for conduction in materials such as PPTh [10]. rGO acts as a conductive pathway to enhance conductivity [32]. When these films are exposed to ammonia/amine vapors, absorbed analyte causes polymer film to swell. This increases interchain distances between neighboring polymer chains. Polymer swelling also disrupts the rGO conductive pathways reducing the conductivity exponentially. The high electronegativity of oxygen atoms in rGO attracts electrons from ammonia and amine functional groups [33] (Figure 7c). This enhances the analyte-trapping ability of the composite film. The combined effect is a much higher sensitivity observed in the case of composite PPTh-rGO films, compared to individual PPTh and rGO films.

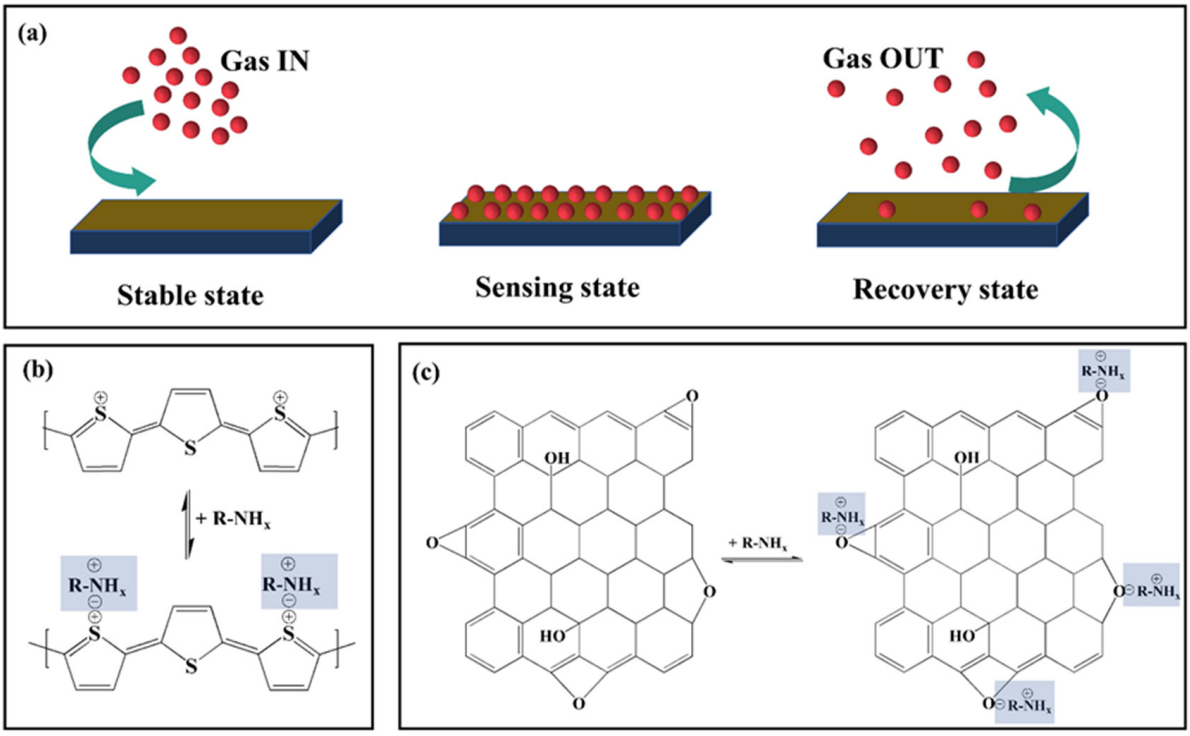

Figure 7. (**a**) Ammonia/amines sensing scheme for PPTh-rGO composite samples, (**b**) Ammonia/amine molecules are absorbed in the film PPTh surface, and (**c**) high electronegativity of oxygen atoms in rGO attracts electrons from ammonia and amine functional groups.

Enhanced selectivity of the PPTh-rGO films is due to the relative polarity of ammonia, MA, DMA, TMA, and other VOCs under study. The high relative polarity of the analyte results in a higher number of molecules being trapped by composite films. On the other hand, lower molecular weights of analyte are preferred by the composite film for maximum trapping [34]. In the case of acetone, benzene, toluene, and dichloromethane, higher molecular weight and lower relative polarities result in lower sensitivity by the PPTh-rGO composite film. Table 4 shows the comparison of previously reported gas sensor studies along with the presented work.

Table 4. Comparison of present work with previously reported similar devices.

Sensing Material	Synthesis Method	Analyte Gas	*Sensitivity*	*Selectivity*	Response/ Recovery Time	Reference
Polythiophene	Chemical synthesis	Methanol—1000 ppm	6.39	~3	~100 s/100 s	[10]
Polythiophene and its derivatives	Oxidative polymerization	Toluene—1000 ppm	42	~8	~100 s/400 s	[11]
Polythiophene	Plasma Polymerization	NO_2—1 ppm	73	NA	1000 s/5000 s	[12]
Functionalized rGO	Chemical synthesis	CO_2—500 ppm	210	NA	60 s/60 s	[35]
rGO	Hummers/Tour's method	Hydrogen—4%	50	NA	~2000 s/1000 s	[36]
PPTh-rGO	Plasma polymerization/Ultrasonic spray deposition	Methylamine—1000 ppm	2354	110	380 s/60 s	Present work
PPTh-rGO	Plasma polymerization/Ultrasonic spray deposition	Ammonia—1000 ppm	2082	97	380 s/60 s	Present work
PPTh-rGO	Plasma polymerization/Ultrasonic spray deposition	Dimethylamine—1000 ppm	1823	85	380 s/60 s	Present work
PPTh-rGO	Plasma polymerization/Ultrasonic spray deposition	Trimethylamine—1000 ppm	1328	62	380 s/60 s	Present work

4. Conclusions

Plasma-polymerized thiophene films were prepared at room temperature using a parallel plate RF plasma polymerization system with varying pulse frequency and duty cycle. PPTh film PT2, with 10 Hz frequency and 10% duty cycle, was optimum for developing sensor films. Composite PPTh-rGO film with PT2 and 1.0 g dispersed in 50 mL water showed the best ammonia/amine gas sensing results. Composite PPTh-rGO film show as much as 4 times ammonia/amine sensing compared to individual PPTh and rGO films. SEM analysis pointed towards reasons for optimized ratios of rGO used with PPTh films for composite formation. FTIR and XRD studies reveal the successful composite formation of PPTh and rGO. PT2G3 sample showed the highest sensitivity for MA, followed by ammonia, DMA, and TMA. PT2G3 showed good repeatability of sensing cycles. It is highly selective for ammonia/amine sensing against several other common VOCs. The calibration curve developed would predict the gas concentration and sensitivity at various concentrations of ammonia/amine. PPTh-rGO composite films showed stable sensitivity for a temperature range of 30 °C to 150 °C. Their sensitivity is found stable for over 4 months. The sensing mechanism predicts polymer swelling, reduction in the number of charge carriers, and disruption of conducting pathways the as a reason for observed ammonia/amine sensitivity of PPTh-rGO composite films.

Supplementary Materials: The following supporting information can be downloaded at: https://www.mdpi.com/article/10.3390/chemosensors11010042/s1, Figure S1: (a) XRD spectra of as-deposited PPTh films PT1, PT2 PT3, and PT4. (b) FTIR spectra of as-deposited PPTh films PT1, PT2, PT3, and PT4; Figure S2: FE-SEM images of (a) PPTh film P2 and (f) rGO powder; SEM images of (a) PT1G3, (b) PT2G3, (c) PT3G3 and (d) PT4G3; Figure S3: Sensing cycles showing the change

in resistance of PPTh-rGO composite PT2G3 for (a) ammonia, (b) MA, (c) DMA and (d) TMA at 1000 ppm each.

Author Contributions: Conceptualization, B.N., P.S.M. and A.u.H.S.R.; Data curation, B.N., Y.B.K., M.U.H.S. and P.S.M.; Formal analysis, Y.B.K., S.F.S., A.T., R.D., P.S.M., A.u.H.S.R. and M.P.; Funding acquisition, S.F.S. and P.S.M.; Investigation, B.N., Y.B.K., S.F.S., A.T., P.S.M., A.u.H.S.R. and M.P.; Methodology, B.N., A.T. and R.D.; Project administration, P.S.M.; Resources, P.S.M., A.u.H.S.R. and M.P.; Software, B.N. and A.T.; Supervision, P.S.M., A.u.H.S.R. and M.P.; Validation, Y.B.K., S.F.S., R.D. and A.u.H.S.R.; Visualization, R.D. and P.S.M.; Writing—original draft, B.N.; Writing—review and editing, Y.B.K., S.F.S., P.S.M., M.U.H.S., A.u.H.S.R. and M.P. All authors have read and agreed to the published version of the manuscript.

Funding: The authors are thankful to the University Grant Commission (UGC) New Delhi, India, for financial support in terms of the major research project and thankful to the Department of Science and Technology (DST) for supporting the Department of Physics, The Institute of Science under the scheme of Fund for Improvement of S & T Infrastructure (FIST). The authors also want to thank Rajiv Gandhi Science and Technology Commission, Mumbai, Maharashtra, for providing financial assistance to this work. (RGSTC/File2016/DPP-146/CR-36). The authors would like to thank the researchers supporting project number (RSP2023R370), King Saud University, Riyadh, Saudi Arabia, for financial support. The authors also sincerely thank KIST School Partnership Project, Seoul, South Korea.

Institutional Review Board Statement: Not applicable.

Informed Consent Statement: Not applicable.

Data Availability Statement: Not applicable.

Conflicts of Interest: The authors declare no conflict of interest.

References

1. Jiang, Y.; Huang, J.; Wang, W.; Hunger, M. Formation of methylamines by the reaction of ammonia with surface methoxy species on zeolite H-Y and the silicoaluminophosphate H-SAPO-34. In *Studies in Surface Science and Catalysis*; Elsevier: Amsterdam, The Netherlands, 2007; pp. 1331–1337.
2. Andre, R.S.; Mercante, L.A.; Facure, M.H.M.; Sanfelice, R.C.; Fugikawa-Santos, L.; Swager, T.M.; Correa, D.S. Recent progress in amine gas sensors for food quality monitoring: Novel architectures for sensing materials and systems. *ACS Sens.* **2022**, *7*, 2104–2131. [CrossRef] [PubMed]
3. Zhang, Y.; Peng, C.; Ma, X.; Che, Y.; Zhao, J. Fluorescent and photoconductive nanoribbons as a dual-mode sensor for selective discrimination of alkyl amines versus aromatic amines. *Chem. Commun.* **2015**, *51*, 15004–15007. [CrossRef] [PubMed]
4. Vasconcelos, H.; Coelho, L.C.C.; Matias, A.; Saraiva, C.; Jorge, P.A.S.; de Almeida, J.M.M.M. Biosensors for biogenic amines: A review. *Biosensors* **2021**, *11*, 82. [CrossRef] [PubMed]
5. Dhall, S.; Mehta, B.R.; Tyagi, A.K.; Sood, K. A review on environmental gas sensors: Materials and technologies. *Sens. Int.* **2021**, *2*, 100116. [CrossRef]
6. Bai, H.; Shi, G. Gas sensors based on conducting polymers. *Sensors* **2007**, *7*, 267–307. [CrossRef]
7. Kawata, K. Development of mass-production-type plasma chemical vapour deposition equipment and its application to various dies. *Surf. Coat. Technol.* **1992**, *54–55*, 604–608. [CrossRef]
8. Lawal, A.T. Graphene-based nano composites and their applications. A review. *Biosens. Bioelectron.* **2019**, *141*, 111384. [CrossRef]
9. Bianco, A.; Cheng, H.-M.; Enoki, T.; Gogotsi, Y.; Hurt, R.H.; Koratkar, N.; Kyotani, T.; Monthioux, M.; Park, C.R.; Tascon, J.M.D.; et al. All in the graphene family—A recommended nomenclature for two-dimensional carbon materials. *Carbon N. Y.* **2013**, *65*, 1–6. [CrossRef]
10. Li, B.; Santhanam, S.; Schultz, L.; Jeffries-EL, M.; Iovu, M.C.; Sauvé, G.; Cooper, J.; Zhang, R.; Revelli, J.C.; Kusne, A.G.; et al. Inkjet printed chemical sensor array based on polythiophene conductive polymers. *Sens. Actuators B Chem.* **2007**, *123*, 651–660. [CrossRef]
11. Gonçalves, V.C.; Balogh, D.T. Optical chemical sensors using polythiophene derivatives as active layer for detection of volatile organic compounds. *Sens. Actuators B Chem.* **2012**, *162*, 307–312. [CrossRef]
12. Park, C.-S.; Kim, D.Y.; Jung, E.Y.; Jang, H.J.; Bae, G.T.; Kim, J.Y.; Shin, B.J.; Lee, H.-K.; Tae, H.-S. Ultrafast Room temperature synthesis of porous polythiophene via atmospheric pressure plasma polymerization technique and its application to NO_2 gas sensors. *Polymers* **2021**, *13*, 1783. [CrossRef] [PubMed]
13. Zhang, R.; Wang, Y.; Li, J.; Zhao, H.; Wang, Y.; Zhou, Y. Mesoporous cellulose nanofibers-interlaced PEDOT:PSS hybrids for chemiresistive ammonia detection. *Microchim. Acta* **2022**, *189*, 308. [CrossRef] [PubMed]

14. Martin, L.; Esteve, J.; Borrós, S. Growth vs. nucleation of conducting polymers thin films obtained by plasma-enhanced chemical vapor deposition. *Thin Solid Films* **2004**, *451–452*, 74–80. [CrossRef]
15. Groenewoud, L.M.H.; Engbers, G.H.M.; White, R.; Feijen, J. On the iodine doping process of plasma polymerised thiophene layers. *Synth. Met.* **2001**, *125*, 429–440. [CrossRef]
16. Geim, A.K.; Novoselov, K.S. The rise of graphene. *Nat. Mater.* **2007**, *6*, 183–191. [CrossRef]
17. Singh, S.A.; More, P.S.; Khollam, Y.B.; Kondawar, S.B. Enhanced Hydrogen gas sensing characteristics of graphene modified with rubidium (Rb). *Mater. Chem. Phys.* **2021**, *260*, 124105. [CrossRef]
18. Mbayachi, V.B.; Ndayiragije, E.; Sammani, T.; Taj, S.; Mbuta, E.R.; Khan, A.U. Graphene synthesis, characterization and its applications: A review. *Results Chem.* **2021**, *3*, 100163. [CrossRef]
19. Madurani, K.A.; Suprapto, S.; Machrita, N.I.; Bahar, S.L.; Illiya, W.; Kurniawan, F. Progress in graphene synthesis and its application: History, challenge and the future outlook for research and industry. *ECS J. Solid State Sci. Technol.* **2020**, *9*, 093013. [CrossRef]
20. Smith, A.T.; LaChance, A.M.; Zeng, S.; Liu, B.; Sun, L. Synthesis, properties, and applications of graphene oxide/reduced graphene oxide and their nanocomposites. *Nano Mater. Sci.* **2019**, *1*, 31–47. [CrossRef]
21. Singh, S.A.; More, P.S.; Late, D.J.; Raut, R.W. Investigation of PEG embedded WO3-graphene thin film sensor. *Adv. Mater. Proc.* **2021**, *2*, 506–509. [CrossRef]
22. More, P.S.; Khollam, Y.B.; Koinkar, P.; Sali, N.D.; Shelke, P.N.; Borwar, S.S. Polyethylene oxide- Cu-composite thick films for lpg sensing. *Int. J. Mod. Phys. B* **2011**, *25*, 4199–4203. [CrossRef]
23. Ben Ishay, R.; Harel, Y.; Lavi, R.; Lellouche, J.-P. Multiple functionalization of tungsten disulfide inorganic nanotubes by covalently grafted conductive polythiophenes. *RSC Adv.* **2016**, *6*, 89585–89598. [CrossRef]
24. Golsheikh, A.M.; Huang, N.M.; Lim, H.N.; Zakaria, R. One-pot sonochemical synthesis of reduced graphene oxide uniformly decorated with ultrafine silver nanoparticles for non-enzymatic detection of H_2O_2 and optical detection of mercury ions. *RSC Adv.* **2014**, *4*, 36401–36411. [CrossRef]
25. Singh, R.; Bajpai, A.K.; Shrivastava, A.K. CdSe nanorod-reinforced Poly(Thiophene) composites in designing energy storage devices: Study of morphology and dielectric behavior. *Polym. Bull.* **2021**, *78*, 115–131. [CrossRef]
26. Gund, G.S.; Dubal, D.P.; Jambure, S.B.; Shinde, S.S.; Lokhande, C.D. Temperature influence on morphological progress of $Ni(OH)_2$ thin films and its subsequent effect on electrochemical supercapacitive properties. *J. Mater. Chem. A Mater.* **2013**, *1*, 4793. [CrossRef]
27. Zhao, Y.-F.; Sun, Y.-P.; Yin, X.; Yin, G.-C.; Wang, X.-M.; Jia, F.-C.; Liu, B. Effect of surfactants on the microstructures of hierarchical sno2 blooming nanoflowers and their gas-sensing properties. *Nanoscale Res. Lett.* **2018**, *13*, 250. [CrossRef] [PubMed]
28. Jeevitha, G.; Abhinayaa, R.; Mangalaraj, D.; Ponpandian, N.; Meena, P.; Mounasamy, V.; Madanagurusamy, S. Porous reduced graphene oxide (RGO)/WO_3 nanocomposites for the enhanced detection of NH_3 at room temperature. *Nanoscale Adv.* **2019**, *1*, 1799–1811. [CrossRef]
29. Wankhede, Y.B.; Kondawar, S.B.; Thakare, S.R.; More, P.S. Synthesis and characterization of silver nanoparticles embedded in polyaniline nanocomposite. *Adv. Mater. Lett.* **2013**, *4*, 89–93. [CrossRef]
30. Potdar, R.P.; Khollam, Y.B.; Shaikh, S.F.; More, P.S.; Rana, A.U.H.S. Polyvinylpyrrolidone-capped silver nanoparticles for highly sensitive and selective optical fiber-based ammonium sensor. *Nanomaterials* **2022**, *12*, 3373. [CrossRef]
31. Postica, V.; Lupan, O.; Gapeeva, A.; Hansen, L.; Khaledialidusti, R.; Mishra, A.K.; Drewes, J.; Kersten, H.; Faupel, F.; Adelung, R.; et al. Improved long-term stability and reduced humidity effect in gas sensing: SiO_2 ultra-thin layered ZnO columnar films. *Adv. Mater. Technol.* **2021**, *6*, 2001137. [CrossRef]
32. Sahu, P.K.; Pandey, R.K.; Dwivedi, R.; Mishra, V.N.; Prakash, R. Polymer/graphene oxide nanocomposite thin film for NO_2 sensor: An in situ investigation of electronic, morphological, structural, and spectroscopic properties. *Sci. Rep.* **2020**, *10*, 2981. [CrossRef] [PubMed]
33. Seekaew, Y.; Lokavee, S.; Phokharatkul, D.; Wisitsoraat, A.; Kerdcharoen, T.; Wongchoosuk, C. Low-cost and flexible printed graphene–PEDOT:PSS gas sensor for ammonia detection. *Org. Electron.* **2014**, *15*, 2971–2981. [CrossRef]
34. Wang, X.; Yong, Y.; Yang, W.; Zhang, A.; Xie, X.; Zhu, P.; Kuang, Y. Adsorption, gas-sensing, and optical properties of molecules on a diazine monolayer: A first-principles study. *ACS Omega* **2021**, *6*, 11418–11426. [CrossRef] [PubMed]
35. Gupta, M.; Hawari, H.F.; Kumar, P.; Burhanudin, Z.A.; Tansu, N. Functionalized reduced graphene oxide thin films for ultrahigh CO_2 gas sensing performance at room temperature. *Nanomaterials* **2021**, *11*, 623. [CrossRef] [PubMed]
36. Drewniak, S.; Procek, M.; Muzyka, R.; Pustelny, T. Comparison of gas sensing properties of reduced graphene oxide obtained by two different methods. *Sensors* **2020**, *20*, 3175. [CrossRef] [PubMed]